Multiconfiguration Dirac-Hartree-Fock calculations of excitation energies, oscillator strengths, and hyperfine structure constants for low-lying levels of Sm I

Fuyang Zhou and Yizhi Qu
College of Material Sciences and Optoelectronic Technology, University of Chinese Academy of Sciences, Beijing 100049, China

Jiguang Li* and Jianguo Wang
Data Center for High Energy Density Physics, Institute of Applied Physics and Computational Mathematics, Beijing 100088, China
(Received 11 June 2015; published 3 November 2015)

The multiconfiguration Dirac-Hartree-Fock method was employed to calculate the total and excitation energies, oscillator strengths, and hyperfine structure constants for low-lying levels of Sm I. In the first-order perturbation approximation, we systematically analyzed correlation effects from individual electrons and electron pairs. It was found that the core correlations are of importance for the physical quantities concerned. Based on the analysis, the important configuration state wave functions were selected to constitute atomic state wave functions. By using this computational model, our excitation energies, oscillator strengths, and hyperfine structure constants are in better agreement with experimental values than earlier theoretical works.

DOI: 10.1103/PhysRevA.92.052505 PACS number(s): 31.15.ve, 31.15.vj, 31.30.Gs

I. INTRODUCTION

The complicated electronic structure of lanthanide atoms leads to unique physical properties which are of great interest to various applications. For example, lanthanide luminescence was investigated for biomedical analyses and imaging in view of their enabling easy spectra and time discrimination of the emission bands which span both the visible and near-infrared ranges [1]. The rich and broad spectra of rare-earth elements are also accessible to astronomy studies [2,3] and have many applications in the lighting community [4]. However, investigation of atomic parameters for rare-earth atoms are quite difficult due to the complicated and strong electron correlation effects mainly arising from electrons in the $4f$ open shell [5–7]. Among the lanthanide atoms, the energy-level structure of samarium is one of the most complex, as shown in Fig. 1 [8]. The term of its ground configuration is [Xe] $4f^6 6s^2\ ^7F$. The open $4f$,$5d$,$6s$, and $6p$ shells in excited states give rise to the complex structure of energy levels, and large overlap between energy blocks can be found from this figure. In this work, we focus on the transitions from configurations $4f^6 6s^2$ to $4f^6 6s 6p$, which contain the lowest states for odd and even parities.

Because of the strong correlation effects, there are only a few *ab initio* calculations of atomic properties for Sm I. Porsev [9] studied the lifetimes of low-lying odd-parity levels $4f^6 6s 6p\ ^9G^o_{0-4}$ and $^9F^o_{1,2}$ within the framework of the relativistic configuration interaction (RCI) method, where electron correlations involving the valence orbitals ($4f$, $5d$, $6s$, and $6p$) were considered. The deviation of their excitation energies from experimental values [10,11] is about 15%, and the calculated oscillator strengths are not consistent with the experimental values [12,13] either. Later, based on the multiconfiguration Dirac-Hartree-Fock (MCDHF) method, Dilip *et al.* [14] investigated the excitation energies and the hyperfine structure (HFS) constants for low-lying levels, where the active space approach was adopted to include the valence correlations involving $5d$, $6s$, and $6p$ electrons. Their excitation energy values are very close to Porsev's values. For HFS, it is interesting that the discrepancy between their results and experimental measurement [15] is considerably large, while the results in the single-configuration approximation by Cheng and Childs [16] agree with experiment quite well. In their calculations, due to the limited computational capacity at that time, the core correlations have not been taken into account, although they were found to be of importance for heavy elements [17].

In this work, we explored the effect of correlation from each electron pair on total energies, excitation energies,and HFS constants for low-lying levels of Sm within the framework of the MCDHF method [18]. On the basis of analysis of electron correlations, the important configurations, accounting for main electron correlations in the first-order perturbation approximation, were selected to calculate the different atomic properties. The agreement between present results and experimental values was dramatically improved by including core correlations.

II. THEORY

In the MCDHF approach, the atomic state wave function (ASF) Ψ is represented as a linear combination of symmetry-adapted configuration state wave functions (CSFs) Φ:

$$\Psi(\Gamma \pi J M) = \sum_r c_\Gamma^r \Phi(\gamma_r \pi J M), \tag{1}$$

where π, J, and M are the parity, total angular momentum, and magnetic quantum number, respectively. Γ and γ_r are the additional quantum numbers to define each ASF or CSF uniquely. Configuration mixing coefficients c_Γ^r are obtained through diagonalization of the Dirac-Coulomb (DC) Hamiltonian

$$H_{\rm DC} = \sum_{i=1}^{N} [c\boldsymbol{\alpha}_i \cdot \boldsymbol{p}_i + (\beta_i - 1)c^2 + V(r_i)] + \sum_{i>j} \frac{1}{r_{ij}}, \tag{2}$$

where the $V(r_i)$ is the monopole part of the electron-nucleus Coulomb interaction, and $\boldsymbol{\alpha}_i$ and β_i are the Dirac matrices. In

*li_jiguang@iapcm.ac.cn

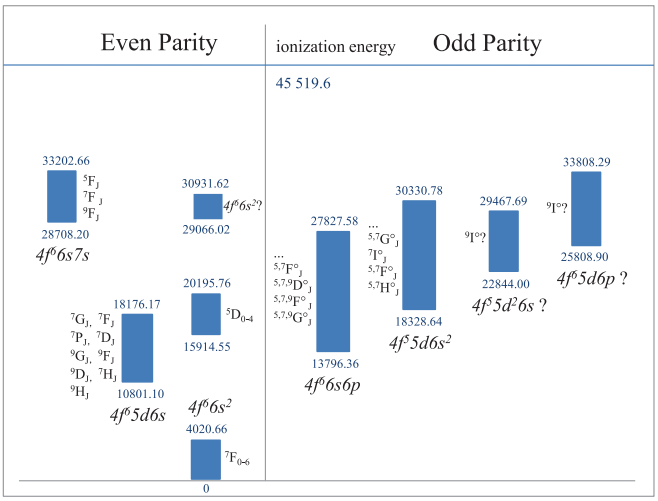

FIG. 1. (Color online) Scheme of the odd-parity and even-parity levels (in cm^{-1}) of the Sm atom.

the relativistic self-consistent field procedure, both the radial parts of Dirac orbitals and the expansion coefficients c_Γ^r are optimized [19].

The Breit interaction in the low-frequency approximation

$$B_{ij} = -\frac{1}{2r_{ij}}\left[\boldsymbol{\alpha}_i \cdot \boldsymbol{\alpha}_j + \frac{(\boldsymbol{\alpha}_i \cdot \boldsymbol{r}_{ij})(\boldsymbol{\alpha}_j \cdot \boldsymbol{r}_{ij})}{r_{ij}^2}\right] \tag{3}$$

and the QED effects including vacuum polarization and self-energy correction can be included in the relativistic configuration interaction computations [20–22].

Once the initial- and final-state wave functions have been obtained, the radiative transition matrix element can be expressed as

$$M_{if} = \langle \Psi(i) \| O^{(1)} \| \Psi(f) \rangle. \tag{4}$$

Here $O^{(1)}$ is the electric dipole ($E1$) interaction. The standard Racah algebra assumes that the orbital sets for the initial- and final-state wave functions are the same [23]. This restriction can be relaxed by the biorthogonal transformation technique [24]. As a result, the transition matrix elements described by independently optimized orbital sets can also be calculated using Racah algebra.

The hyperfine structure of the atomic energy levels is caused by electromagnetic interactions between the nucleus and electrons. The magnetic dipole ($M1$) and electric quadrupole ($E2$) hyperfine interaction constants A and B are given by [25]

$$A_J = \frac{\mu_I}{I}\frac{1}{[J(J+1)]^{1/2}}\langle \Gamma_J J \| \boldsymbol{T}^{(1)} \| \Gamma_J J \rangle \tag{5}$$

and

$$B_J = 2Q_I\left[\frac{J(2J-1)}{(J+1)(2J+3)}\right]\langle \Gamma_J J \| \boldsymbol{T}^{(2)} \| \Gamma_J J \rangle. \tag{6}$$

Here, I is the nuclear spin, μ_I is the nuclear magnetic dipole moment, Q_I is the nuclear quadrupole moment, and $\boldsymbol{T}^{(k)}$ is the electronic tensor operators of rank k. The $M1$ and $E2$ hyperfine operators $\boldsymbol{T}^{(1)}$ and $\boldsymbol{T}^{(2)}$ are defined as [25], in atomic units,

$$\boldsymbol{T}^{(1)} = \sum_{j=1}^{N} \boldsymbol{t}^{(1)}(j) = -i\alpha(\boldsymbol{\alpha}_j \cdot \mathbf{1}_j \boldsymbol{C}^{(1)}(j)) r_j^{-2} \tag{7}$$

and

$$\boldsymbol{T}^{(2)} = \sum_{j=1}^{N} \boldsymbol{t}^{(2)}(j) = -\boldsymbol{C}^{(2)}(j) r_j^{-3}, \tag{8}$$

where α is the fine-structure constant, and $\boldsymbol{C}^{(k)}$ is the spherical tensor operator of rank k.

In this work, the new version of the GRASP2K package [20] was adopted to calculate wave functions and atomic properties, such as excitation energies, oscillator strengths, and HFS constants.

III. ELECTRON CORRELATION EFFECTS

In the multiconfiguration calculations, one can obtain the indication of the important correlation corrections according to the perturbation theory [19,26]. The zero-order ASF should include the dominant configuration state functions. The first-order correction of ASFs is composed of all CSFs which interact with zero-order ASFs and thus can be expressed as a linear combination of CSFs that are obtained by single and double (SD) substitutions from occupied orbitals of the reference configuration to virtual orbitals. The first-order correlations can be further classified into different pair correlations which are defined by all possible substitutions from a certain electron pair [19]. Based on determination of the contributions from each pair correlation, the important correlation corrections can be selected effectively to investigate atomic quantities.

In this work, we are concerned with the low-lying levels of Sm I, the ground configuration of which is [Xe] $4f^6 6s^2$, and the lowest odd-parity levels belong to the [Xe] $4f^6 6s 6p$ configuration. The $4f$, $6s$, and $6p$ orbitals were treated as valence, and the others were core orbitals. Due to the huge CSF space arising from the open $4f$ shell, the first-order correlation effects (especially for the excited state) could not be completely included within our computational capacity. Therefore, we divided them into several subsets from individual electrons or electron pairs, the contributions from which could be evaluated in a series of smaller configuration-interaction (CI) calculations. The analysis of the first-order electron correlations for the ground and excited states proceeded as follows:

(1) The occupied orbitals were optimized as spectroscopic in the single-configuration approximation and kept frozen in subsequent calculations. The relaxation effect was accounted for by the independent optimization of the ground and excited states.

(2) The virtual orbitals were generated in a restricted configuration space, in which only some electron-pair correlations were included in the MCDHF approach. For example, in the relativistic self-consistent field procedure, the configurations could be obtained by SD substitutions from valence orbitals to the virtual ones. As a result, these virtual orbitals were optimized to accommodate the contributions from only valence correlations.

TABLE I. Correlation energy ΔE for ground state $4f^6 6s^2\ ^7F_0$. Model: SrD, MCDHF calculations with the configurations were obtained by all single and restricted double (SrD) substitutions to these virtual orbitals (the restriction was described in text); SD, CI calculations with configurations were generated by single and unrestricted double (SD) replacement. Layers indicate number of virtual orbitals of a particular symmetry. NCF is the number of CSFs with $J = 0,1,2$. $E(^7F_1 - ^7F_0)$ is the excitation energy in cm^{-1} of $^7F_1 - ^7F_0$.

Model	Layers	NCF	ΔE (cm^{-1})	$E(^7F_1 - ^7F_0)$
SrD	"1$spdfg$"	9 152	−27 078.48	298.16
SrD	"2$spdfg$"	18 164	−28 712.10	302.47
SrD	"3$spdfg$"	27 176	−28 913.40	303.75
SD	"3$spdfg$"	322 280	−32 115.94	307.40
	Experiment [5]			292.58

(3) By applying the orbitals generated above, the different electron correlation effects could be included in a series of CI calculations to select the important ones.

(4) The Breit and QED corrections were estimated in the single-configuration approximation.

In the evaluations of various atomic properties, the important configuration state wave functions were selected on the basis of analysis of electron correlation effects. Moreover, we could optimize the orbitals to accommodate the contributions from the selected electron correlations in the framework of the MCDHF method.

A. Generation of the virtual orbitals

In the present MCDHF approach, to reduce complexity of self-consistent field calculations the virtual orbitals were added layer by layer. The configurations were obtained by single and restricted double (SrD) substitutions from valence orbitals, in which the two occupied orbitals must be replaced by two of the same virtual orbitals; i.e., only the double substitutions from $4f$, $6s$, and $6p$ to virtual orbitals nl^2 were permitted. The one-electron energy values of virtual orbitals do not have physical meaning; the properties of virtual orbitals depend on the correlation effects they describe [27]. In this paper the virtual orbitals were enclosed in quotation marks to avoid confusion with occupied orbitals, and they are listed by angular symmetry and quantity. For example, "2$spd1f$" means two of each of the s, p, and d symmetries and one of the f symmetry.

In this section, three virtual layers for levels with even parity and two virtual layers for ones with odd parity were generated within the framework of the MCDHF method. In order to check the validity of this restriction on double substitutions, contributions from the reduced configurations were added in the CI calculation, where the configurations were obtained by single and unrestricted double (SD) substitutions from valence orbitals to all virtual orbitals generated above.

Tables I and II present the correlation energies for the ground state $4f^6 6s^2\ ^7F_0$ and the excited state $4f^6 6s6p\ ^9G_0^o$, as well as the excitation energies of $4f^6 6s^2\ ^7F_1$ and $4f^6 6s6p\ ^9G_0^o$ states. The correlation energy is defined as the total energy difference between the multiconfiguration and single-configuration values. As can be seen from Table I, the calculations with one virtual layer could capture most of the valence correlation effects for the ground state. In addition, the SrD model can include the valence correlation effects effectively with a smaller number of CSFs. For example, the difference in ΔE between the SrD and SD models is 3196 cm^{-1} for the ground state and 3.74 cm^{-1} in the fine structure of the $^7F_1$ level, while the NCF was reduced to 27 176 from 322 280.

TABLE II. Correlation energy ΔE for exited state $4f^6 6s6p\ ^9G_0^o$. NCF is the number of CSFs with $J = 0,1$. $E(^9G_0^o - ^7F_0)$ is the excitation energy in cm^{-1} of $^9G_0^o - ^7F_0$.

Model	Layers	NCF	ΔE (cm^{-1})	$E(^9G_0^o - ^7F_0)$
SrD	"1$spdfg$"	51 017	−23 559.04	10 234.69
SrD	"2$spdfg$"	100 370	−25 654.01	9 773.33
SD	"2$spdfg$"	457 452	−27 549.98	10 394.95
	Experiment [5]			13 796.36

Similar results for the excited state were given in Table II, in which the total and excitation energies were not significantly improved by the expansion of configuration space. However, the excitation energies $E(^9G_0^o - ^7F_0)$ differ from the experimental value by more than 3000 cm^{-1}. Therefore, the contributions from the electron correlations which were not included in the generation of virtual orbitals should be evaluated.

B. Contributions from different electron correlations

In order to include the significant correlations with respect to computational capacity, we divided the one- and two-body electron correlations into several subsets. The CI approach was used to include different correlation effects within the virtual orbital set "1$spdfg$", in which orbitals generated above were applied and kept frozen. For example, the valence correlation of $4f^6 6s6p$ could be divided into $4f$, $6s$, $6p$, $4f^2$, $4f6s$, $4f6p$, and $6s6p$ electron correlations. The $4f$ electron correlation effect was expressed as a linear combination of CSFs that are obtained by single replacement $4f \rightarrow v$ (virtual orbital), and the CSFs for the $4f6s$ electron pair correlation were obtained by unrestricted double replacement $4f6s \rightarrow vv'$. Based on these CI calculations, the contributions from each correlation subset to the total energy were evaluated by the absolute value of correlation energies ΔE.

1. Valence correlations

The contributions from the different valence correlations to the total energy E_0 of the ground state $4f^6 6s^2\ ^7F_0$ and the excited state $4f^6 6s6p\ ^9G_0^o$ (E_1) are presented in Fig. 2. For the ground-state total energy E_0, the individual electron correlations are $4f$, $6s$, $4f^2$, $4f6s$, and $6s^2$. It was found that the one-body correlation effects from valence orbitals are negligible. The most important valence correlation is from the $4f^2$ electron pair, while the contributions from the $6s^2$ and $4f6s$ pair correlations to the correlation energies are much smaller than it.

The contributions of the specific correlation effects for the excited state are similar to that for the ground state. The one-body correlations also have a negligible effect on the

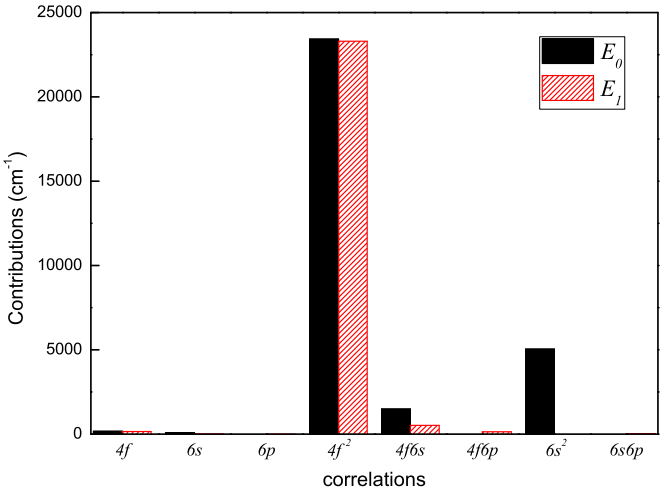

FIG. 2. (Color online) Contributions from the different valence correlation effects to the total energies for ground state $4f^6 6s^2\ ^7F_0$ (E_0) and exited state $4f^6 6s6p\ ^9G^o_0$ (E_1). The contributions were evaluated by the absolute value of correlation energies ΔE.

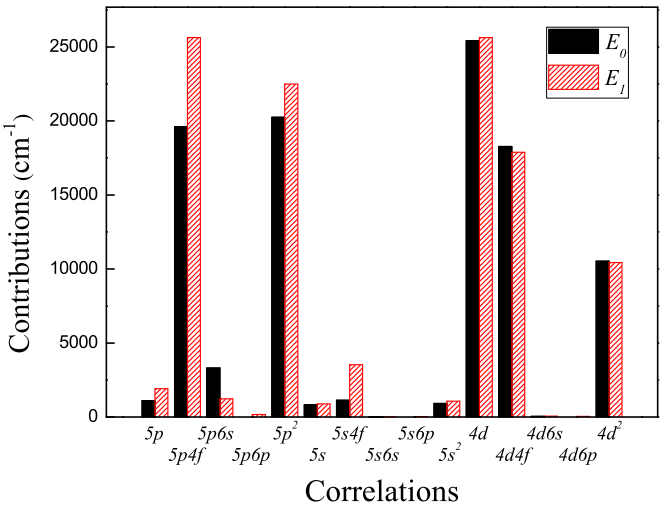

FIG. 3. (Color online) Contributions from the different electron correlation effects involving core shells $4d5s5p$ to total energies for ground state (E_0) and exited state (E_1).

total energy E_1. The most important valence correlation is from $4f^2$ electron pair, and the $4f6s$ and $4f6p$ correlations contribute little to the total energy. This result indicates that the electrostatic interaction between the deep-lying $4f$ electron and outer $6s$ and $6p$ electrons is very weak.

Although essentially important for the total energies, it was found that the correlation between $4f^2$ electrons has only a small influence on the excitation energy $E(^9G^o_0 - ^7F_0)$. The change in excitation energy $E(^9G^o_0 - ^7F_0)$ mostly comes from the difference of electron correlation effects involving the external $6s6p$ and $6s^2$ electrons. This could also be due to the weak interaction between the $4f$ electron and outer electrons.

The excitation energy $E(^9G^o_0 - ^7F_0)$ calculated with these valence-valence (VV) correlations is 10 394.95 cm^{-1} (see Table II), compared with the experimental value of 13 796.36 cm^{-1}. Apart from the valence correlation effects, there are other types of correlation effects involving the core shells. The difference of 3000 cm^{-1} should come from the core-valence (CV) and core-core (CC) correlation effects.

2. *Correlations involving core shells*

In Fig. 3 we present the contributions from the different correlations involving core shells $4d5s5p$ to the total energy E_0 for the ground state $4f^6 6s^2\ ^7F_0$ and the exited state $4f^6 6s6p\ ^9G^o_0$ (E_1). The contributions from one-body correlations are quite small except for the $4d$ electron. In addition, the CV correlation effects between core and $4f$ electrons, especially for the $5p4f$ and $4d4f$ electron pair correlations, are very important to the total energy E_0. For CC correlations, only the nl^2 pair correlation effects were illustrated in the figure because they are more important than correlations between electrons in different orbitals; e.g., the contributions from $5p^2$ and $4d^2$ pair correlations exceeded 10 000 cm^{-1}. These correlations involving $4d$ and $5p$ shells strongly influence the atomic state wave functions. The one- and two-body correlation effects involving $3spd4sp$ shells were also taken into account for the ground state, but their contributions are much smaller than $4d5s5p$ shells.

For the exited state, due to the huge CSF space arising from the reference configuration $4f^6 6s6p$, only CV and the most important part of CC correlations (i.e., the nl^2 pair correlations) were considered. The effects of electron correlations involving $4d5sp$ shells to the total energy are similar to the ground state $^7F_0$. The $5p4f$, $4d4f$, $5p^2$, and $4f^2$ electron pair correlation effects are most important, and the contributions from the correlations between the core and the $6p$ electrons are even smaller than $6s$ pair correlations.

As can be seen from Fig. 3, the correlations involving $5p$ and $5s$ electrons have a significant influence on the excitation energy $E(^9G^o_0 - ^7F_0)$. However, it seems that these core correlations would decrease the $E(^9G^o_0 - ^7F_0)$, while the result without core correlations lowers the experimental value by about 3000 cm^{-1}. This could be because the convergence in the present CI calculations was slowed down by the fact that the virtual orbitals were optimized to accommodate the contributions from only valence correlations.

In order to obtain reasonable contributions from the correlation effects involving $5p$ and $5s$ electrons to the excitation energy, we have reoptimized the virtual orbitals in MCDHF calculations with the inclusion of electron correlations involving core orbitals $5s$ and $5p$, respectively. In Fig. 4 we present the contributions from these electron correlation effects to the total energy for the ground state (E_0) and the exited state (E_1) with the new set of virtual orbitals. The contributions to the total energy are similar to those using the previous orbital set; that is, the $5p4f$ and $5p^2$ electron correlation effects are most significant. However, the $5p4f$ and $5p^2$ pair correlations have a negligible influence on the excitation energy. Additionally, the correlations between $5p$ and external $6s$ and $6p$ electrons are most important to the excitation energy. For the $5s$ electron, the contribution from the $5s4f$ correlation to the excitation energy is also very small, and the correlations between $5s$ and outer $6s6p$ electrons have a negligible effect on both total and excitation energies.

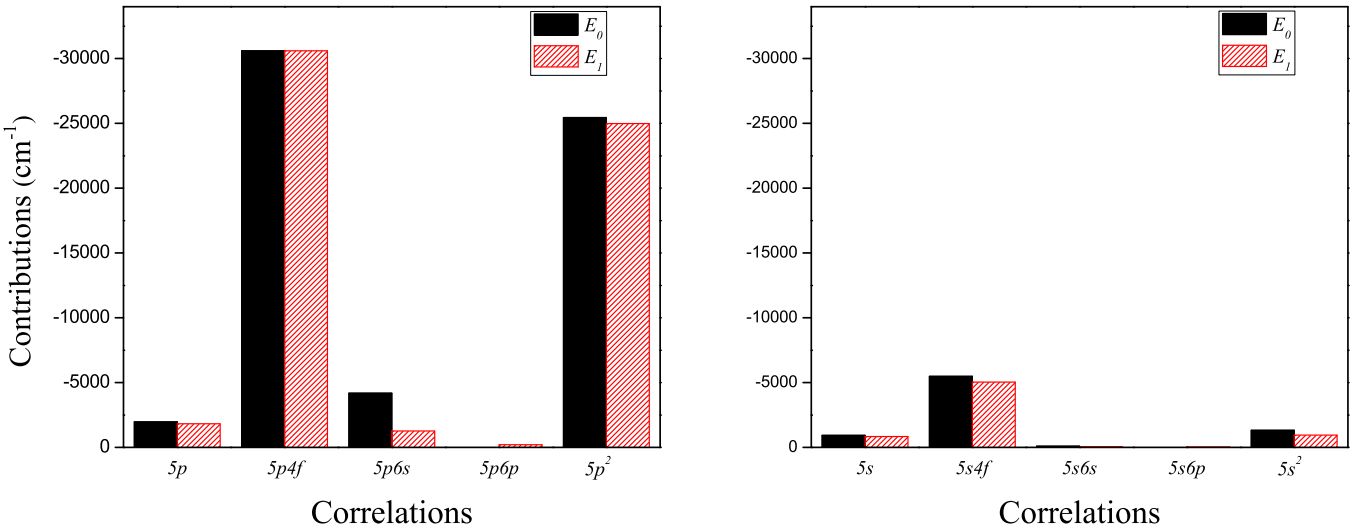

FIG. 4. (Color online) Contributions from the different correlation effects involving $5p$ and $5s$ electrons to total energies for ground state (E_0) and exited state (E_1). In order to obtain accurate contributions for the analysis on excitation energy, the virtual orbitals are reoptimized to accommodate the correlations involving $5p$ and $5s$ electrons, respectively. See text for further details.

These individual contributions indicate that the core correlations are very important for total energies. For the excitation energy $E(^9G_0^o - ^7F_0)$, the CV correlation effects from $5p$ electrons were found to be significant and tended to improve the result without core correlation.

C. Breit and QED corrections

In Table III we display the excitation energies of $4f^6 6s6p$ $^9G^o_{0,1}$ and $^9F^o_1$ states, as well as the correction of Breit interaction and QED effects in the single-configuration approximation. It was found that these high-order corrections have a negligible effect on excitation energies. The remaining discrepancy between calculations and experimental values is mostly attributed to the electron correlations involving core shells which are not included.

IV. CALCULATION OF ATOMIC PROPERTIES

A. Excitation energies and oscillator strengths

1. Calculational model

As mentioned above, the first-order correlations could not be adequately included in the calculations for Sm with respect to the open $4f$ shell that results in a huge CSF space. In order to carry out an accurate calculation of the excitation energies and transition probabilities, the important specific correlations should be selected to form the ground and excited atomic state wave functions, based on analysis of electron correlation effects. Also, the orbitals need to be optimized to accommodate the contributions from the selected electron correlations in the framework of the MCDHF method.

As discussed in Sec. III, the valence correlations involving outer $6s$ and $6p$ electrons should be included in this correlation model, which significantly influence the excitation energy. Apart from the valence correlation, the CV correlations were found to be very important as well. Therefore, in our MCDHF calculations, the $4f6s$, $4f6p$, $6s^2$, $6s6p$, $5p6s$, and $5p6p$ electron pair correlations should be included.

For the transitions from $4f^6 6s6p$ $^9G^o_1$ and $^9F^o_1$ to $4f^6 6s^2$ $^7F_{0,1,2}$, the levels belonging to the lower and upper configurations were optimized in two separate MCDHF calculations. At the starting point, the occupied orbitals were obtained in the single-configuration approximation. Then we extended our calculations to include the selected correlations, which further included the important core correlations compared with the calculations in Table II. The CSFs were obtained by single and double substitutions from the selected electron pair to virtual orbitals. Although a larger virtual orbital set is more conducive to including the selected correlations, only the "$2spd1f$" virtual orbitals were generated in our calculation due to the large size of CSFs. The number of CSFs within this computational model is given in Table IV. The configuration space is considerably smaller than the one generated by the conventional active space approach. For example, the number of CSFs with this correlation model for the $^9G^o_1$ and $^9F^o_1$ state is 291 689, compared to 20 701 402 CSFs obtained by SD substitutions from orbitals $4df5sp6sp$ to the same orbital set.

TABLE III. Breit and QED effect on the excitation energies of $4f^6 6s6p$ $^9G^o_{0,1}$ and $^9F^o_1$ states of Sm in cm^{-1}. DHF indicates the uncorrelated Dirac-Hartree-Fock calculation, and VV indicates the multiconfiguration calculation with valence-valence correlations.

Model	$^9G^o_0 - ^7F_0$	$^9G^o_1 - ^7F_0$	$^9F^o_1 - ^7F_0$
DHF	6 694	6 899	7 944
VV	10 394.95	10 601.49	11 624.21
Breit correction	–67	–89	–77
Breit and QED correction	–114	–136	–124
Experiment [5]	13 796.36	13 999.50	14 863.85

2. Results

The transition energies and oscillator strengths of transitions from $4f^6 6s6p$ $^9G^o_1$ and $^9F^o_1$ to $4f^6 6s^2$ $^7F_{0,1,2}$ states for different configuration models are presented in Table V

TABLE IV. The number of CSFs as a function of the virtual orbital set in the MCDHF calculations with this correlation model (described in Sec. IV A 1): "*nspdf*", virtual orbital set; J^P, total angular momentum (J) and parity (P) of an atomic state.

Model	$J^P = 1^o$	$J^P = 0^e$	$J^P = 1^e$	$J^P = 2^e$
Single configuration	252	14	19	37
"1*spdf*"	113 231	2280	10 440	23 220
"2*spd*1*f*"	291 689	5087	26 120	60 421

and compared with other theoretical and experimental data. The large discrepancy between single-configuration results and experimental values indicates that the strong electron correlation effects exist in Sm I. Due to the computational limitation at that time, only part of the VV correlation could be included in Porsev's CI calculation [9], and Porsev's results of transition energies are about 2000 cm^{-1} lower than experimental data. The present multiconfiguration approach gave much better results. For example, the excitation energy of $4f^6 6s6p\ ^9G_1^o$ was improved to 14 265 cm^{-1}, only 266 cm^{-1} higher than the experimental value. This result indicates that this correlation model could account for the major difference of the electron correlation effects between ground and exited states.

The oscillator strengths in Babushkin (length) and Coulomb (velocity) gauges (f_B, f_C) for transitions from $4f^6 6s6p\ ^9G_1^o$ and $^9F_1^o$ to $4f^6 6s^2\ ^7F_{0,1,2}$ states are also given in Table V. It can be seen that the electron correlation effects on the oscillator strengths are remarkable. Compared with Porsev's results, the oscillator strengths in the Babushkin gauge agree well with experimental data, and the agreement was improved with increase of configuration space. For the $^9F_1^o$-$^7F_{0,1}$ transitions, which have the largest transition probabilities, the deviations are less than 10% from the experimental values. However, the transition rates for weak lines are less accurate than those for strong lines, since the values are too small and thus more sensitive to electron correlation effects, especially for the $^9G_1^o$-$^7F_1$ transition.

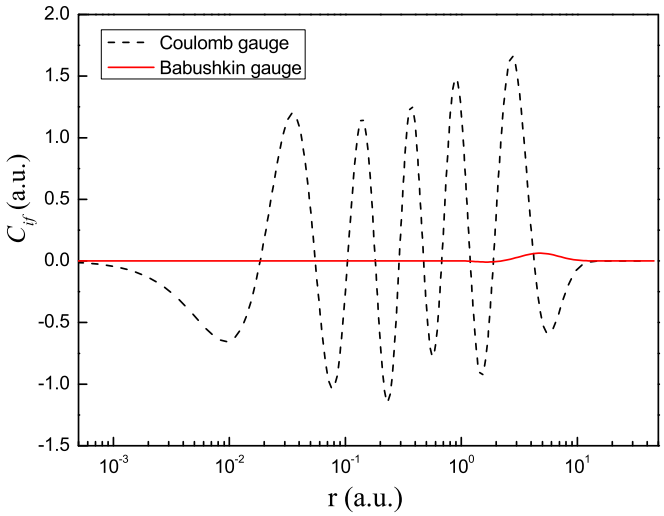

FIG. 5. (Color online) Radial distribution of the transition matrix element $\langle {}^7F_0 \| O^{(1)} \| {}^9G_1^o \rangle$ in Coulomb and Babushkin gauges.

Meanwhile, we noted that the inconsistency in the oscillator strengths between different gauges is very large. The oscillator strengths in the Coulomb gauge are much larger than those in the Babushkin gauge. The gauge difference is ascribed to the fact that the $E1$ transition amplitudes in Babushkin and Coulomb gauges are sensitive to different radial regions of the wave functions. Therefore, we defined a radial-dependent factor $C_{if}(r)$ by

$$M_{if} = \int_0^\infty C_{if}(r)dr, \tag{9}$$

where M_{if} is the radiative transition matrix element. In Fig. 5, we illustrate the radial dependence of $C_{if}(r)$ for the transition matrix element $\langle {}^7F_0 | O^{(1)} | {}^9G_1^o \rangle$ in Babushkin and Coulomb gauges. It was found that only the wave function in the larger r region contributes significantly to the $E1$ transition amplitude in the Babushkin gauge, while the transition matrix element in the Coulomb gauge is very sensitive to the whole region

TABLE V. Excitation energies E (in cm^{-1}) and oscillator strengths f (10^{-4}) for $E1$ transitions from odd-parity $^9G_1^o$ and $^9F_1^o$ states to even-parity $^7F_{0-2}$ states: B, Babushkin gauge; C, Coulomb gauge; "*nspdf*", virtual orbital set of the MCDHF calculation with the correlation model described in Sec. IV A 1.

	$^9G_1^o$-$^7F_0$				$^9G_1^o$-$^7F_1$				$^9G_1^o$-$^7F_2$			
Model	E	f_B	f_C	f_B/f_C	ΔE	f_B	f_C	f_B/f_C	E	f_B	f_C	f_B/f_C
Single configuration	6 899	1.66	0.07	42	6 621	0.01	0.02	0.45	6107	0.60	0.01	63
"1*spdf*"	13 087	16.35	61.3	0.27	12819	10^{-6}	0.03	$3*10^{-5}$	12305	7.56	33.4	0.23
"2*spd*1*f*"	14 265	11.05	22.7	0.49	14001	0.006	0.03	0.24	13488	4.01	9.46	0.42
Porsev [9]	11 533	6.9[a]			11248	0.1[a]			10723	2.8[a]		
Experiment [10,13]	13 999.50	12.5			13 706.92				13 187.58	5.7		
	$^9F_1^o$-$^7F_0$				$^9F_1^o$-$^7F_1$				$^9F_1^o$-$^7F_2$			
Model	ΔE	f_B	f_C	f_B/f_C	E	f_B	f_C	f_B/f_C	ΔE	f_B	f_C	f_B/f_C
Single configuration	7944	4.07	1.34	3.03	7665	5.70	3.42	1.7	7151	1.47	1.98	0.74
"1*spdf*"	14127	46.4	134.3	0.35	13859	42.2	118.9	0.35	13345	4.66	10.7	0.44
"2*spd*1*f*"	15291	27.8	47.6	0.58	15026	34.2	57.7	0.59	14514	6.54	10.0	0.65
Porsev [9]	12674	19.6[a]			12389	30[a]			11864	9.0[a]		
Experiment [10,13]	14863.85	28.2			14571.21	31.7			14051.93			

[a] $f = f_B E_{expt}/E_{th}$.

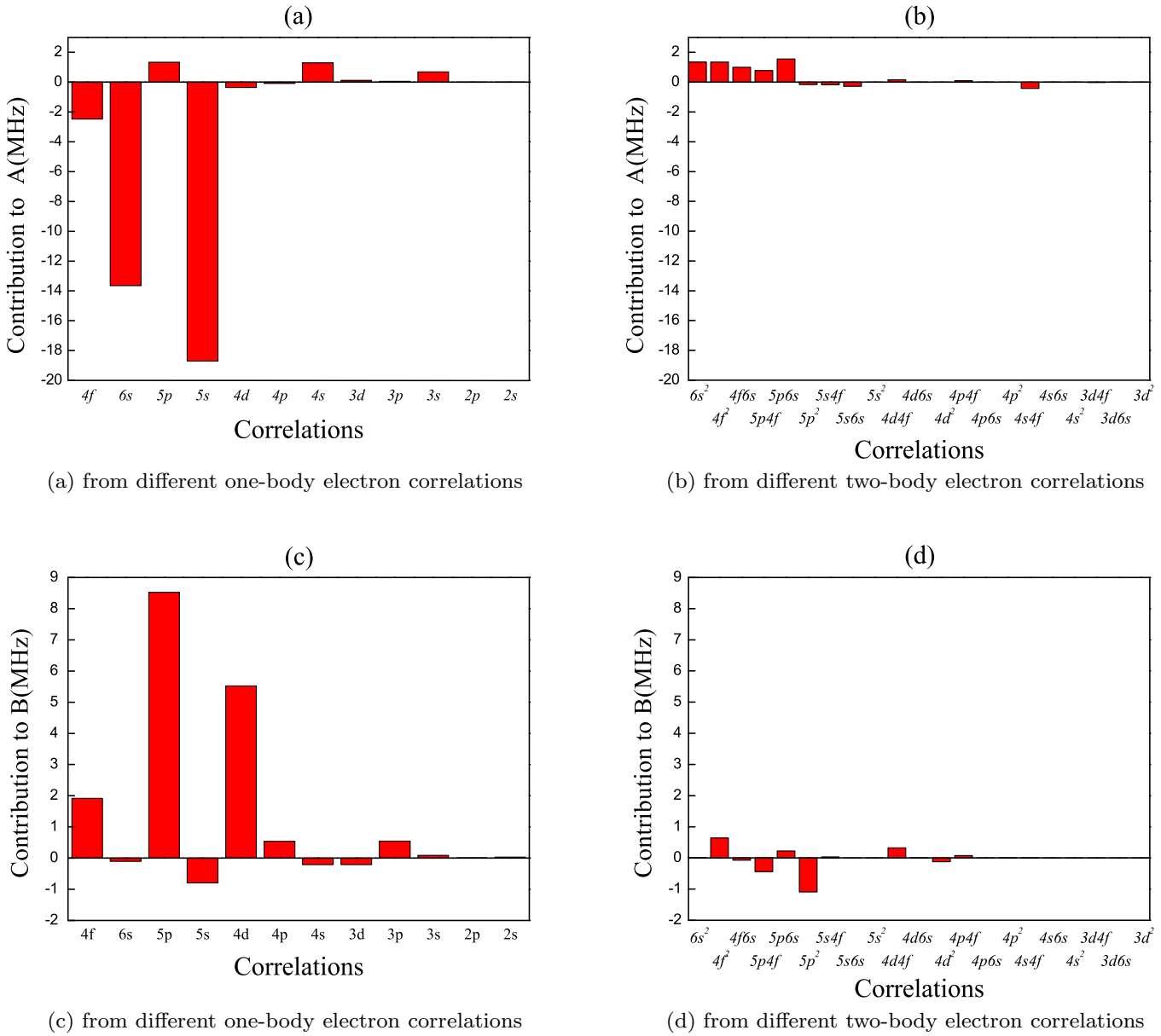

(a) from different one-body electron correlations

(b) from different two-body electron correlations

(c) from different one-body electron correlations

(d) from different two-body electron correlations

FIG. 6. (Color online) Contributions from different one- and two-body electron correlation effects to HFS constants A and B of the $4f^6 6s^2\ {}^7F_1$ state. The contributions were evaluated by the difference between the multiconfiguration and single-configuration values.

of wave functions. Meanwhile, there are large cancellations in the integral of the transition matrix element in the Coulomb gauge, which lead to the requirement of higher-quality wave functions. As a result, the oscillator strengths in the Babushkin gauge are more reliable than the ones in the Coulomb gauge.

In this work, only the selected first-order electron correlations were taken into account in the calculations. The uncertainties of the transition energies and oscillator strengths are mainly attributed to the higher-order and the residual first-order electron correlations. The comparison with the experimental data presented in Table V can give us a rough estimate of the uncertainties of our results. Approximately, the errors in the present calculations of the transition energies are 2–3 %. For the oscillator strengths, the differences between the results in the Babushkin gauge and experimental values are about 30% for the ${}^9G^o_1$ -${}^7F_2$ transition, and 10% for the stronger lines. Next, we examine the influence of different correlation models on the HFS constants.

B. The hyperfine constants

Atomic HFS provides an important test for *ab initio* atomic-structure calculation, since hyperfine interactions are sensitive to electron correlations. Cheng and Childs calculated the ground-state multiplet HFS constants of the Sm atom within the single-configuration approximation [16]. The results are in quite good agreement with experiment [15]. Later, a multiconfiguration calculation was reported by Dilip *et al.* [14] with worse results compared with experimental values. In view of this, we investigated different electron correlation effects on HFS constants and then carried out new multiconfiguration calculations for the $4f^6 6s^2\ {}^7F_1$ state.

TABLE VI. The hyperfine constants A, B, and B/Q for the $^7F_1$ state of ^{147}Sm. VV, multiconfiguration calculation with valence-valence correlations; "$nspdfg$", virtual orbital set of the MCDHF calculation with the correlation model described in Sec. IV B; $\mu = -0.812\mu_N$ and $Q = -0.261b$ were taken from Ref. [28].

Model	A (MHz)	B (MHz)	B/Q (MHz/b)
Single configuration	−33.73	−75.89	290.77
"1$spdfg$"	−99.45	−26.22	100.46
"2$spdfg$"	−30.77	−60.19	230.61
"3$spdfg$"	−31.89	−60.88	233.26
Dilip [14]	−23.12	−35.70	
Cheng [16]	−33.77	−58.88[a]	290.05
Experiment [15]	−33.493	−58.688	224.86

[a]Calculated with $Q = -0.203b$.

In Fig. 6, we present the contributions from the different correlations to the magnetic dipole HFS constants A and electric quadrupole constant B of the $4f^6 6s^2\ ^7F_1$ state for the ^{147}Sm isotope with nuclear spin $I = 7/2$. Using the experimental nuclear parameters taken from Ref. [28], the contributions were evaluated by the difference between the multiconfiguration and single-configuration values. It was found that the one-body electron correlations are very important to the constants, since the major corrections for hyperfine interaction are the spin and orbital polarizations [19]. The two-body electron correlations have a relatively smaller effect on the HFS constants, although they are essentially important for the total energy. Therefore, in our MCDHF calculations the one-body electron correlations from $3spd4spdf5sp6s$ shells were chosen to form atomic state wave functions.

Using the computational model described above, the HFS constants A, B, and B/Q of the $4f^6 6s^2\ ^7F_1$ state for the ^{147}Sm isotope are presented in Table VI. In the single-configuration approximation, our result for the constant A agrees with the similar work of Cheng and Childs [16] and experimental measurement [15] quite well. Reference [16] provides a better result for constant B, but they used a fitting electric quadrupole moment Q. The similar B/Q results from Ref. [16] and ours are given in this table. In our multiconfiguration calculations, the HFS constants A and B were significantly changed by the considered electron correlations, and then they were converged with the expansion of the configuration space. The results of both constants A and B have a good agreement with experimental data. Moreover, the constant B was improved from the single-configuration calculation, only about 2 MHz lower than the experimental value. The large discrepancies between Dilip *et al.*'s multiconfiguration calculation [14] and experimental data could be because they only partly considered VV correlations, which could not improve the results when the electron correlation effects balance out.

For the exited state, there are no theoretical predictions of HFS according to the best of our knowledge. Using the same computational model, the results of the HFS constants for $4f^6 6s6p\ ^9F^o_1$ and $^7G^o_1$ states are shown in Table VII. In this case, the single-configuration calculations could not provide reasonable results. For example, the calculated HFS constant B of the $^7G^o_1$ state is 10.79 MHz while the experimental value is −9.63 MHz [29]. Although our MCDHF calculations of HFS constant A were not fully converged, the values of constant B were largely improved by the captured one-body correlation effects. The constant B of the $^7G^o_1$ state becomes −12.49 MHz, much closer to the experimental value.

TABLE VII. The hyperfine constants A and B for $4f^6 6s6p\ ^9F^o_1$ and $^7G^o_1$ states of ^{147}Sm: "$nspdf$", virtual orbital set.

	$^9F^o_1$		$^7G^o_1$	
Model	A (MHz)	B (MHz)	A (MHz)	B (MHz)
Single configuration	−241.05	19.24	−171.83	10.79
"1$spdf$"	−539.05	17.27	−89.22	−14.11
"2$spdf$"	−326.12	15.86	−169.75	−12.49
Experiment [29]	−423.34	13.21	−212.62	−9.63

In our calculations of hyperfine constants, only the one-body electron correlations were considered. All the two-body correlations and the higher-order corrections contribute to the uncertainties. However, the errors of both constants A and B of the $4f^6 6s^2\ ^7F_1$ state were found to be less than 5%. For the $4f^6 6s6p\ ^9F^o_1$ and $^7G^o_1$ states, the accuracy of the results mainly depended on the convergence of the calculations. Comparing with experimental values, the deviation of the hyperfine constants of $^9F^o_1$ and $^7G^o_1$ states are about 20–30 %.

V. CONCLUSION

Recently, the partitioned correlation function interaction (PCFI) approach was developed for complicated atoms [30,31], which relaxes the orthonormality restriction on the orbital basis and breaks down the originally very large calculations into a series of smaller calculations. The subspace of CFSs makes it easier to capture the effects weakly connected to total energy, which could be significant for some atomic properties. For the calculations of a complicated atom like Sm, with complicated and strong electron correlation effects, it would be very useful to divide the electron correlations. In this work, we also divided the first-order electron correlations into several subsets, but we used the MCDHF method to investigate these correlation effects on total energies, excitation energies, and HFS constants. It was found that the core correlations are of importance for the total energies. However, only the correlations involving $6s$ and $6p$ valence orbitals significantly influence the excitation energies, although they make relatively small contributions to total energies. For HFS constants, the major corrections are from the one-body electron correlation effects.

Based on the analysis of electron correlation effects, the important configuration state wave functions were selected to calculate the different atomic properties using the MCDHF approach. The results of transition energies and oscillator strengths from $4f^6 6s6p\ ^9G^o_1$ and $^9F^o_1$ to $4f^6 6s^2\ ^7F_{0,1,2}$ states have a much better agreement with experiment, compared with previous calculations without core correlations. Furthermore, the HFS constants were also calculated for examining correlation models. It was found that the validity of the single-configuration approximation is restricted on ground-state multiplets and more complicated electron correlations are required for treating the HFS for excited states. By including the important correlation effects, the reasonable results were obtained for $4f^6 6s6p\ ^9F^o_1$ and $^7G^o_1$ and $4f^6 6s^2\ ^7F_1$ states.

ACKNOWLEDGMENTS

We would like to thank Professor Per Jönsson for his helpful discussions. This work was supported by the NSAF (Grant No. U1330117), the National Natural Science Foundation of China (Grant No. 11404025), and the China Postdoctoral Science Foundation (Grant No. 2014M560061).

[1] J.-C. G. Bünzli, Chem. Rev. **110**, 2729 (2010).
[2] J. E. Lawler, C. Sneden, J. J. Cowan, I. I. Ivans, and E. A. Den Hartog, Astrophys. J. Suppl. Ser. **182**, 51 (2009).
[3] C. Sneden, J. E. Lawler, J. J. Cowan, I. I. Ivans, and E. A. Den Hartog, Astrophys. J. Suppl. Ser. **182**, 80 (2009).
[4] J.-C. G. Bünzli and C. Piguet, Chem. Soc. Rev. **34**, 1048 (2005).
[5] W. C. Martin, R. Zalubas, and L. Hagan, *Atomic Energy Levels: The Rare-Earth Elements* Natl. Bur. Stand. Ref. Data Ser., Natl. Bur. Stand. (U.S.) Circ. No. NBS-60,422 (U.S. GPO, Washington, D.C., 1978).
[6] D. R. Beck and E. Domeier, Can. J. Phys. **87**, 75 (2009).
[7] D. R. Beck and S. M. O'Malley, J. Phys. B **43**, 215003 (2010).
[8] A. Kramida, Yu. Ralchenko, J. Reader, and NIST ASD Team, NIST Atomic Spectra Database (ver. 5.2) (NIST, Gaithersburg, MD, 2014), `http://physics.nist.gov/asd`.
[9] S. G. Porsev, Phys. Rev. A **56**, 3535 (1997).
[10] K. B. Blagoev, V. A. Komarovskii, and N. P. Penkin, Opt. Spektrosk. **42**, 424 (1977).
[11] J. E. Lawler, A. J. Fittante, and E. A. Den Hartog, J. Phys. B **46**, 215004 (2013).
[12] V. A. Komarovskii and Y. M. Smirnov, Opt. Spektrosk. **80**, 357 (1996).
[13] V. A. Komarovskii, N. P. Penkin, and G. P. Nikiforova, Opt. Spektrosk. **29**, 220 (1970).
[14] A. Dilip, I. Endo, A. Fukumi, M. Iinuma, T. Kondo, and T. Takahashi, Eur. Phys. J. D **14**, 271 (2001).
[15] W. Childs and L. Goodman, Phys. Rev. A **6**, 2011 (1972).
[16] K. T. Cheng and W. J. Childs, Phys. Rev. A **31**, 2775 (1985).
[17] Y. Zou and C. F. Fischer, Phys. Rev. Lett. **88**, 183001 (2002).
[18] I. P. Grant, *Relativistic Quantum Theory of Atoms and Molecules* (Springer, New York, 2007).
[19] C. F. Fischer, T. Brage, and P. Jönsson, *Computational Atomic Structure: An MCHF Approach* (Institute of Physics Publishing, London, 1997).
[20] P. Jönsson, G. Gaigalas, J. Bieroń, C. Froese Fischer, and I. Grant, Comput. Phys. Commun. **184**, 2197 (2013).
[21] P. Jönsson, X. He, C. Froese Fischer, and I. Grant, Comput. Phys. Commun. **177**, 597 (2007).
[22] F. Parpia, C. Froese Fischer, and I. Grant, Comput. Phys. Commun. **94**, 249 (1996).
[23] U. Fano, Phys. Rev. **140**, A67 (1965).
[24] J. Olsen, M. R. Godefroid, P. Jönsson, P. A. Malmqvist, and C. F. Fischer, Phys. Rev. E **52**, 4499 (1995).
[25] P. Jönsson, F. Parpia, and C. Froese Fischer, Comput. Phys. Commun. **96**, 301 (1996).
[26] J. G. Li, P. Jönsson, M. Godefroid, C. Z. Dong, and G. Gaigalas, Phys. Rev. A **86**, 052523 (2012).
[27] J. Bieroń, C. Froese Fischer, P. Indelicato, P. Jönsson, and P. Pyykkö, Phys. Rev. A **79**, 052502 (2009).
[28] N. Stone, At. Data Nucl. Data Tables **90**, 75 (2005).
[29] H. Park, M. Lee, and Y. Rhee, J. Korean Phys. Soc. **43**, 336 (2003).
[30] C. Froese Fischer, S. Verdebout, M. Godefroid, P. Rynkun, P. Jönsson, and G. Gaigalas, Phys. Rev. A **88**, 062506 (2013).
[31] S. Verdebout, P. Rynkun, P. Jönsson, G. Gaigalas, C. Froese Fischer, and M. Godefroid, J. Phys. B **46**, 085003 (2013).